



Department of Physics

ASTM-052: Extragalactic Astrophysics

by

Peter Clegg

**Note 2. General Properties
of Galaxies**

Table of Contents

Note 2 : GENERAL PROPERTIES OF GALAXIES	1
1. Introduction	1
2. Morphological Classification.....	1
2.1 Hubble's Classification.....	1
2.2 Elliptical Galaxies.....	1
2.3 Spiral Galaxies.....	3
2.4 Lenticular Galaxies.....	3
2.5 Irregular Galaxies	4
2.6 Dwarf Galaxies.....	4
2.7 Peculiar and Interacting Galaxies	4
3. Photometry of Galaxies	5
3.1 Surface Photometry	5
3.2 Use of Magnitudes.....	6
3.2.1 Definition of Magnitude	6
3.2.2 Surface Brightness	6
3.2.3 Magnitude Systems.....	6
3.2.4 Colours	7
3.2.5 The Magnitudes of Galaxies.....	7
3.3 Photometry of Elliptical Galaxies.....	8
3.4 Photometry of Spiral Galaxies.....	9
3.5 Colours of Galaxies	10
4. Masses of Galaxies	10
4.1 Introduction	10
4.2 Photometric Methods.....	11
7.2.1 Mass-Luminosity Ratios for Stars	11
4.2.1 Stellar Mass-Function.....	11
4.3 Spectroscopic Methods.....	12
7.2.1 Physical Basis.....	12
4.3.1 The Virial Theorem	12
4.3.2 Masses of Elliptical Galaxies.....	12
4.3.3 Masses of Spiral Galaxies.....	14
4.4 Mass-Luminosity Ratios for Galaxies	16
Bibliography for Note 2.....	16

NOTE 2: GENERAL PROPERTIES OF GALAXIES

1. Introduction

Galaxies show a wide range of sizes, shapes and properties. In this chapter I shall first discuss the classification of galaxies according to their optical shapes and will go on to discuss some of their more general properties. I shall return to some of these properties later for more specific discussion.

2. Morphological Classification

2.1 Hubble's Classification

There are many schemes for classifying galaxies, even if we confine ourselves to those schemes based on optical appearances. Which scheme one should adopt depends largely on what one wants to do with the classification. For many purposes, and certainly for ours in this course, Hubble's morphological classification is adequate.

On the basis of their appearance, Hubble split galaxies into two groups, regular and irregular (Irr). He divided the regular galaxies into two basic types, elliptical (E) and spiral (S). The class of spirals was additionally divided into ordinary (SA, but more usually just S) and barred (SB) galaxies. This scheme is shown in Hubble's tuning-fork diagram of Figure 2-1.

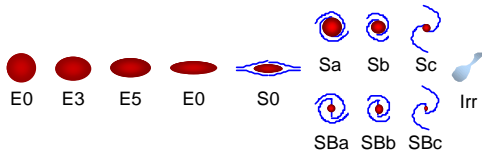


Figure 2-1 Hubble's Classification Scheme

I emphasise that the sequence is merely one of classification and, although it reflects different origins and histories for the various classes of object, it certainly does *not* represent the evolutionary track of an individual galaxy.

2.2 Elliptical Galaxies

The class of ellipticals is sub-divided into a sequence numbered from 0 to 7 according to the ellipticity of the shape of the galaxy as projected on to the plane of the sky. This is also, of course, its shape on a photographic plate or CCD. In general an elliptical is classed as E_n where n is given by

$$n = \text{ROUND} \left[10 \times \left(\frac{a-b}{a} \right), 0 \right] \tag{2.1}$$

$$= \text{ROUND} \left[10 \times \left(1 - \frac{b}{a} \right), 0 \right],$$

where a and b are the semi-major and semi-minor axis of the image respectively, and $\text{ROUND}[x,r]$ denotes that the quantity x is to be rounded to r decimal places. The ellipticity e of the image is defined by

$$e := 1 - \frac{b}{a} \tag{2.2}$$

so that

$$n = \text{ROUND}[10e,0] \tag{2.3}$$

Figure 2-2 shows the giant E0 galaxy M87.



Figure 2-2 AA Telescope image of the giant elliptical galaxy M87 (NGC 4486). [Copyright AAO/ROE].

It is important to realise that what we see is the *projection* of the true shape of a galaxy on to the plane of the sky. We automatically tend to adjust for this when looking at images of spiral galaxies. We assume, with good reason as I shall show later, that the “disc” part of a spiral galaxy is basically circular and that, if it appears elongated, that is because it is tilted to our line-of-sight. In the case of an elliptical galaxy, however, we tend to think of the shape of the projected image as being the shape of the galaxy itself. This may not be true. If an elliptical galaxy were shaped like a rugby ball, for example, its image would be circular if its long axis were aligned along the line of sight. Similarly, a rugby-ball shaped galaxy aligned in this way would be classified as an E0 galaxy,

Could all “elliptical” galaxies be flat-ish discs, their ellipticity merely being a projection effect? Perhaps they are merely spiral galaxies with no nuclear bulge (see below) viewed at various angles so that an E0 galaxy would a bulge-less spiral observed face on. Let us test this hypothesis¹.

Consider Figure 2-1, which shows a disc of radius a and thickness c inclined at an angle θ to the line of sight to an observer. It is easy to show that, for c equal to zero, the projected image of the disc appears to the observer

¹ This is a useful demonstration of the use of statistical arguments in astronomy.

as an ellipse with semi-major axis a and semi-minor axis b , where

$$b = a \cos \theta, \tag{2.4}$$

so that

$$e = 1 - \cos \theta. \tag{2.5}$$

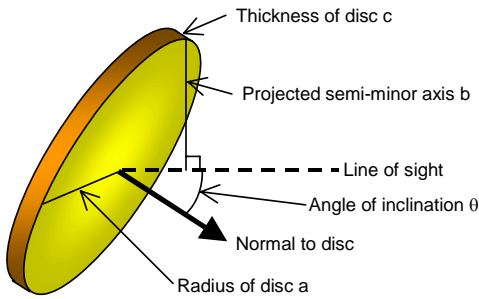


Figure 2-3. A thin disc model of ellipticals.

If c is non-zero, the image is no longer an ellipse. It is nevertheless easy to show - try it! - that the effective value e' of the ellipticity, defined as unity minus the ratio of the maximum thickness t to the width w of the image (cf. Figure 2-4) is given by

$$e' := 1 - \frac{t}{w} = 1 - \frac{b + c \sin \theta}{a} \tag{2.6}$$

$$= 1 - \cos \theta - \frac{c}{a} \sin \theta.$$

The maximum value of e for a thick disc is therefore $1 - c/a$ and occurs when $\theta = \pi/2$.

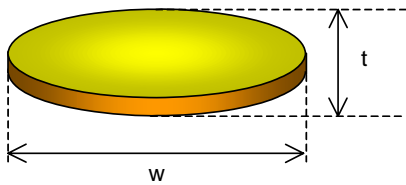


Figure 2-4. Aspect ratio of disc.

The simplest argument against the hypothesis is that the flattest ellipticals are E7, corresponding to a value of 0.3 for c/a . This is very much greater than the observed value for the discs of spirals. Alternatively, we should have to suppose that all ellipticals conspire to be inclined by no more than about 75° (cf. exercise) to our line of sight, an unlikely state of affairs.

A more detailed argument involves the observed frequency distribution of ellipticals amongst the various classes. Let us assume that the orientation of the hypothetical flat discs is random. Then the normal to the disc shown in Figure 2-5 can point in any direction. What is the probability of its pointing in the range of

angles θ to $\theta + d\theta$ as shown? Ignore for the moment the thickness of the disc. Let the length of the normal be r . Then the area dA of the annulus on the circumscribed sphere between θ to $\theta + d\theta$ is given by

$$dA = 2\pi r \sin \theta \times r d\theta. \tag{2.7}$$

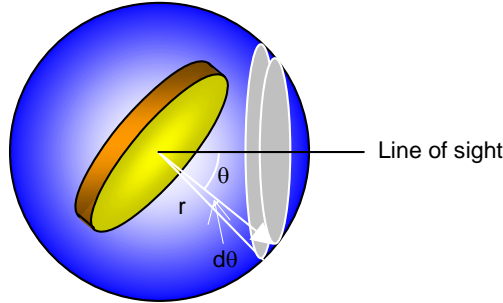


Figure 2-5. Alignment geometry.

The total surface area A of the hemisphere into which the normal can point² is $2\pi r^2$ so that the probability $dP(\theta)$ of its being in the above range of angles is given by

$$dP(\theta) = \frac{dA}{A} = \frac{2\pi r^2 \sin \theta d\theta}{2\pi r^2} = \sin \theta d\theta. \tag{2.8}$$

From equation (2.6), with c set equal to zero, we have

$$de' = \sin \theta d\theta \tag{2.9}$$

so that, from equation (2.8),

$$dP(\theta) = de'. \tag{2.10}$$

The probability $dP(e')$ of the observed value of e falling in the range e' to $e' + de'$ is given by

$$dP(e') = dP(\theta) = de', \tag{2.11}$$

where I have used equation (2.10).

Equation (2.11) says that, if elliptical galaxies were thin discs, we should expect a uniform distribution of ellipticities; if they were thick discs, we should expect the relationship to hold until the inclination was such that the second term in equation (2.6) became important, that is at high ellipticities.

Figure 2-6 shows schematically the observed numbers of galaxies as a function of ellipticity e . It is quite clear that the distribution of ellipticals does not follow the horizontal line expected of discs and that it cuts off at E7. It must therefore be accepted that elliptical galaxies

²Note that we only have to consider θ in the range 0 to $\pi/2$ because values greater than this simply mean that we are looking at the disc from the (presumably identical) other side.

are truly ellipsoidal in form³. But we find that, even within the class of ellipsoids there are tri-axial ellipsoids, oblate ellipsoids, prolate ellipsoids and spheroids; the image of the galaxy will not help us to decide on the shape of any particular galaxy. An E0 galaxy, for example, cannot be the projection of a tri-axial ellipsoid but it could be prolate, oblate – viewed along the symmetry axis – or truly spheroidal.

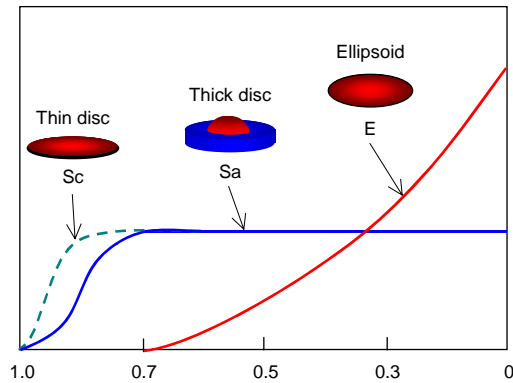


Figure 2-6. Observed distribution of ellipticities.

2.3 Spiral Galaxies

Although spiral galaxies are named after the structure that is so dramatically evident, the name does not convey the overall structure of these galaxies in the same way as does the name elliptical. The images of spiral galaxies consist of two main components, a disc (which is correctly inferred to be flat) and a nuclear bulge⁴. A better name for these galaxies is *disc galaxies*.

As indicated in Figure 2-1, each branch (S and SB) of the spiral sequence is further sub-divided into a sequence running from *a* to *c*.



Figure 2-7. AAT photograph of the Sc spiral galaxy NGC 2997. [Copyright AAO]

³ It can be shown that the projection of any ellipsoid on to a plane is an ellipse, regardless of the angle of projection.

⁴ I shall show later that there are other components, which are not as obvious.

Figure 2-7 shows the Sc (or SAc) galaxy NGC 2997 whilst Figure 2-8 shows the SBb galaxy NGC 1365



Figure 2-8. AAT photograph of the SBb barred spiral galaxy NGC 1365. [Copyright AAO]

As might be expected, there are also intermediate cases such as Sab, a spiral between Sa and Sb, or SABB, a spiral halfway between a barred and unbarred spiral at position b in the sequence.

The assignment of a place in the sequence depends upon the relative sizes of the bulge and disc components: the bigger the bulge relative to the disc, the earlier⁵ in the sequence is the galaxy put. Some Sc and SBc galaxies have almost non-existent bulges. Strongly correlated with the bulge-to-disc ratio is the tightness of winding of the spiral arms in the disc. Earlier Hubble types have tightly wound arms, later types much more open arms, as indicated schematically in Figure 2-1. There is also a correlation between the luminosity of a spiral and how well the arms are defined. Van den Bergh defined luminosity classes I – luminous with well-defined arms, to V – weaker with patchy arms. We shall see later that this correlation fits with our understanding of how spiral arms are formed.

Figure 2-6 shows schematically the distribution of the ellipticity of the imaged discs of Sa and Sc spirals. Until the inclination becomes so large that the thickness of the disc begins to play a part, as predicted by equation (2.6), these curves obviously *do* follow the expected distribution for discs. You will also see from the curves that Sc galaxies have thinner discs than Sa galaxies, as also indicated in the figure.

2.4 Lenticular Galaxies

Figure 2-9 is an image of the galaxy NGC 1201, which looks rather like an elliptical but which has faint extensions of its long axis. Detailed photometry (see later) reveals that the isophotes – contours of constant surface brightness – of this galaxy are elliptical towards the centre but becomes open curves towards the edges, as sketched in Figure 2-1 for the object labelled S0.

⁵ Note the word “early” is not to be interpreted in terms of time but of the position of a galaxy in the Hubble sequence, going from left to right.

Comment [PEC1]: Get original data.

These open isophotes suggest the vestiges of a disc-like structure viewed nearly edge on, although there is no evidence of spiral structure. Such *lenticular* galaxies are therefore in some sense intermediate between the most elongated ellipticals, E7, and true spirals. Some S0 galaxies show evidence of a bar-like structure and may be classified as SB0.

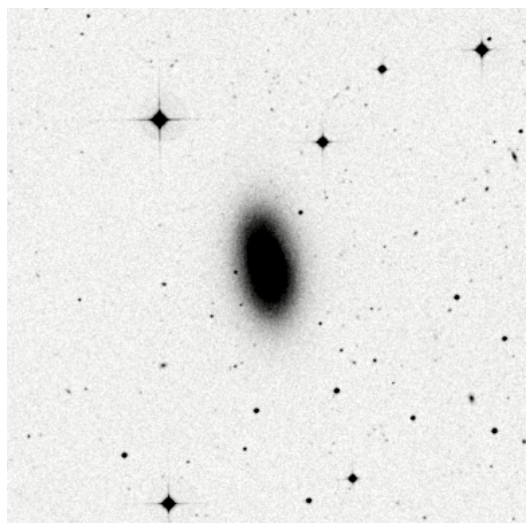


Figure 2-9. UKS image of the S0 galaxy NGC 1201. [Copyright AAO]

2.5 Irregular Galaxies

Hubble classified as irregular (Irr) those galaxies that appeared to have no recognisable form. We now distinguish two types of irregulars, IrrI [or Irr(m)] which look irregular but in which the distribution of material is rather regular, and IrrII [or Irr(o)] which really are irregular! An example of an IrrI, which accounts for the alternative designation, is the Large Magellanic Cloud (LMC), shown in Figure 2-10. The LMC has weak spiral structure and a bar.



Figure 2-10. AAT photograph of the LMC. [Copyright AAO/ROE]

IrrI galaxies may be thought of as an extension of the Hubble sequence of spiral galaxies to the point where

the nuclear bulge is non-existent and the arms so loose that the structure becomes almost unrecognisable. Indeed, de Vaucouleurs inserts an Sd class between Sc and IrrI. Irregulars are, therefore, sometimes put at the right-hand end of the tuning-fork diagram, as in Figure 2-1.



Figure 2-11. KPNO 0.9m image of the irregular galaxy M82. [Copyright Association of Universities for Research in Astronomy Inc. (AURA)]

Copyright Association of Universities for Research in Astronomy Inc. (AURA), all rights reserved

Type IrrII is well illustrated by the galaxy M82, shown in Figure 2-11, which has almost certainly collided with its companion M81, resulting in massive star formation. I shall return to this sort of object later.

2.6 Dwarf Galaxies

The most numerous galaxies are dwarf ellipticals (dE) and dwarf irregulars (dIrr), as we shall see. There are no dwarf spirals

2.7 Peculiar and Interacting Galaxies

A number of galaxies did not fit conveniently into any of the classes discussed above; Hubble called these peculiar. Peculiar galaxies are not a well-defined class. Moreover, some galaxies which are classified as E or S have peculiarities associated with them and are designated (p), e.g. E0(p). I shall not deal with the entirety of peculiar galaxies; some will arise when I deal with active galaxies in a later chapter.

Of particular current interest, however, are interacting galaxies. Figure 2-12 is a Hubble Space Telescope true-colour image of the Cartwheel Galaxy, located 150 Mpc away in the constellation Sculptor. We think that the ring-like structure is the result of a smaller galaxy, perhaps one of the two objects to the right of the ring, passing right through the core of the Cartwheel. The effect of the impact would have been to create an expanding “ripple” in the interstellar medium, leaving massive star-formation behind it. This is traced by the blue knots containing hot young stars and by the loops and bubbles of gas created by supernovae.

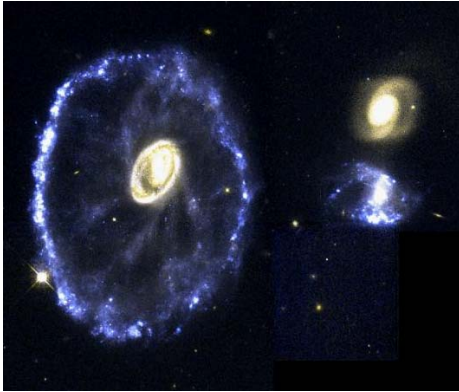


Figure 2-12. Cartwheel galaxy. [Copyright Kirk Borne (ST ScI), and NASA]

The Cartwheel was probably a normal spiral prior to the collision and spiral structure is beginning to re-emerge in the form of faint “spokes”.

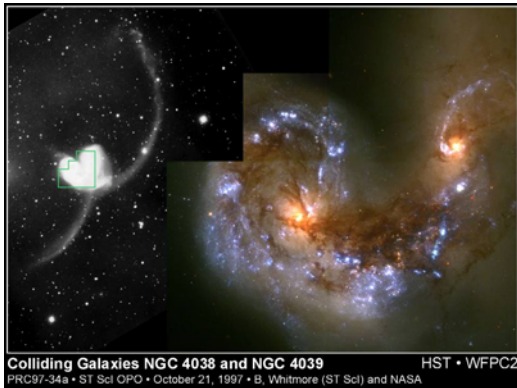


Figure 2-13. The Antennae. [Copyright AURA]

Figure 2-13 is another example of interaction between galaxies and shows the effects of a close encounter between two galaxies on star-formation. These galaxies have also been studied in detail by the *Infrared Astronomy Satellite (ISO)*, which has revealed more detail of the sites of star formation.

Studies of such interactions can help us understand the processes of star formation in more normal situations. An example is the origin of globular clusters. As the Space Telescope Science Institute press release [1] said, “These spectacular images are helping us understand how globular star clusters formed from giant hydrogen clouds in space,” [says] Francois Schweizer of the Carnegie Institution of Washington, Washington, D.C. “This galaxy is an excellent laboratory for studying the formation of stars and star clusters since it is the nearest and youngest example of a pair of colliding galaxies.” ... Globular star clusters are not necessarily relics of the earliest generations of stars formed in a galaxy, as once commonly thought, but may also provide fossil records of more recent collisions.”

3. Photometry of Galaxies

3.1 Surface Photometry

If we are to understand what is going on in galaxies, we certainly need to know how much power they radiate in all regions of the electromagnetic spectrum. I shall concentrate on optical wavelengths in this section and return to other regions of the spectrum later in the course. We are interested both in the total power generated and in how this generation is distributed throughout the galaxy, the latter being particularly important in trying to model the galaxy's *density profile*. Photometry of galaxies is difficult and the results are hard to interpret; I shall only outline those results that are of direct relevance to the course.

Consider a source which radiates a total power L ; we call L the *luminosity* of the source. Assuming for the moment that this power is radiated isotropically (the same in all directions), then at the distance r of the Earth from the source, this power is spread uniformly over a sphere of area $4\pi r^2$. The power per unit area, or *flux density* F , received by an observer at the Earth is therefore given by

$$F = \frac{L}{4\pi r^2}. \tag{2.12}$$

The *surface brightness* or intensity I of the galaxy is defined as the flux-density received per unit solid angle Ω of the source:

$$I := \frac{dF}{d\Omega}. \tag{2.13}$$

In general, I will depend on the angular position (θ, ϕ) , in some suitable set of co-ordinates, of the part of the galaxy we are looking at.

If we know $I(\theta, \phi)$, we can in principle estimate the total flux density emitted by the galaxy. From equation (2.13), we have

$$F = \int_{\text{galaxy}} I(\theta, \phi) d\Omega. \tag{2.14}$$

The “edges” of galaxies are very poorly defined, however, and this estimate is prone to considerable error as we shall see shortly.

We can see that the intensity of a source is independent of its distance. For consider a small element of the surface of the source with area dA which has luminosity dL and subtends an angle $d\Omega$ at the Earth. Then

$$dA = r^2 d\Omega. \tag{2.15}$$

From equation (2.12), this element emits flux density dF , where

$$dF = \frac{dL}{4\pi r^2} \quad (2.16)$$

so that, from (2.13),

$$I(\theta, \phi) \equiv \frac{dF}{d\Omega} = \frac{dL}{dA}, \quad (2.17)$$

which is independent of r .

So far I have not specified any particular wavelength range over which the intensity, flux density or luminosity are measured. If we measure over the whole range of wavelengths at which the emission is important, we speak of *bolometric* quantities Q_{bol} , like F_{bol} for example. More usually, we are concerned with the emission over a restricted band of wavelengths and we use quantities Q_{λ} , where the amount dQ of Q emitted in the wavelength range λ to $\lambda+d\lambda$ is given by

$$dQ = Q_{\lambda} d\lambda. \quad (2.18)$$

The relationship between Q_{bol} and Q_{λ} is

$$Q_{\text{bol}} = \int_{\text{all wavelengths}} Q_{\lambda} d\lambda. \quad (2.19)$$

3.2 Use of Magnitudes

3.2.1 DEFINITION OF MAGNITUDE

For historical reasons, astronomers usually use magnitudes for expressing the values of optical flux density. The magnitude m of a source with flux density F is defined by

$$m = -2.5 \log \left(\frac{F}{F_o} \right) \quad (2.20)$$

where F_o is some standard flux-density. Note the negative sign in the definition, which means that the *more* luminous the source, the *smaller* (algebraically) is its magnitude. If a source at distance r has luminosity L , we have from equations (2.6) and (2.20),

$$m = -2.5 \log \left(\frac{L}{4\pi r^2 F_o} \right). \quad (2.21)$$

The *absolute magnitude* M of a source is defined to be the magnitude it would have if it were at a distance r_{10} equal to 10 parsecs. From equation (2.10), therefore,

$$M = -2.5 \log \left(\frac{L}{4\pi r_{10}^2 F_o} \right) \quad (2.22)$$

From equations (2.11) and (2.6), we have an expression for the distance r of the source in terms of its *distance modulus* $m-M$:

$$\begin{aligned} m - M &= -2.5 \log \left(\frac{r_{10}^2}{r^2} \right) = 5 \log \left(\frac{r}{r_o} \right) \\ &= 5 \log \left[\frac{r(\text{pc})}{10} \right] = 5 \log [r(\text{pc})] - 5. \end{aligned} \quad (2.23)$$

3.2.2 SURFACE BRIGHTNESS

In terms of magnitudes, surface brightness μ is expressed, rather confusingly, in *magnitudes per unit standard solid angle*:

$$\mu(\theta, \phi) = -2.5 \log \left[\frac{I(\theta, \phi)}{I_o} \right] \quad (2.24)$$

where I_o is the intensity corresponding to F_o in some standard solid angle Ω_o :

$$I_o = \frac{F_o}{\Omega_o}. \quad (2.25)$$

Note that, just as I is independent of the distance of the source (equation (2.17)), so is μ . The standard solid angle is chosen as 1 arcsec² and the brightness μ is expressed in *magnitudes per square arcsec*. This terminology is misleading! Because of the logarithmic relationship between μ and I , the total magnitude of a galaxy is NOT given by the integral of $\mu(\theta, \phi)$ over the angular extent of the galaxy:

$$m \neq \int_{\text{galaxy}} \mu(\theta, \phi) d\Omega.$$

We have, rather, that

$$m = -2.5 \log \left[\frac{I_o}{F_o} \int_{\text{galaxy}} 10^{-0.4\mu(\theta, \phi)} d\Omega \right]. \quad (2.26)$$

3.2.3 MAGNITUDE SYSTEMS

As with quantities such as brightness or luminosity, we can either use the bolometric magnitude m_{bol} or, more usually, the magnitude m_{λ} at some particular wavelength λ :

$$m_{\lambda} = -2.5 \log \left(\frac{F_{\lambda}}{F_{o\lambda}} \right) \quad (2.27)$$

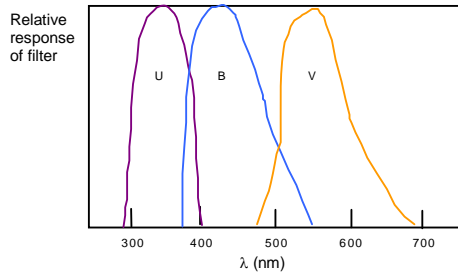


Figure 2-14. The U, B and V filters.

The most common system is the *UBV* system in which magnitudes are measured using a set of in the U (ltraviolet), B (lue), V (isual) bands, as shown schematically in Figure 2-14. The central wavelengths λ_o , bandwidths $\Delta\lambda$ and standard flux-densities $F_{o\lambda}$ are given in Table 2-1.

Table 2-1 The *UBV* system.

Magnitude	m_U	m_B	m_V
Symbol	U	B	V
λ_o (μm)	0.365	0.440	0.550
$\Delta\lambda$ (μm)			
$F_{o\lambda}$ (Jy)	19	43	38
1 Jy = 10^{-26} W m ⁻² Hz ⁻¹			

3.2.4 COLOURS

The colour of an object between two wavelengths λ_1 and λ_2 is defined as the difference $m_{\lambda_1} - m_{\lambda_2}$ in the magnitudes of the object at those two wavelengths. From equation (2.27), we have

$$m_{\lambda_1} - m_{\lambda_2} = -2.5 \left[\log \left(\frac{F_{\lambda_1}}{F_{\lambda_2}} \right) - \log \left(\frac{F_{o\lambda_1}}{F_{o\lambda_2}} \right) \right] \quad (2.28)$$

so that the colour is a measure of the ratio of the flux-densities at the two wavelengths. The colour of gives us a (rather crude) measure of the spectrum of the object. That of a star tells us its spectral type, which itself depends upon the mass and age of the star. Hence the colours of galaxies can tell us about the ages of their stellar populations.

The colours deriving from the *UBV* system are (*U-B*) and (*B-V*). Notice that, because of the negative sign in the definition of the magnitude, the *smaller* algebraically its values of (*U-B*) or (*V-B*), the *more* ultraviolet or blue, respectively, an object is.

3.2.5 THE MAGNITUDES OF GALAXIES

Because galaxies have ill-defined edges, it is difficult to decide where to stop in such integrations as those in equations (2.8) or (2.26). Astronomers therefore often use other, more or less arbitrary ways of estimating the total magnitude of a galaxy. The *metric magnitude* is the flux within an aperture of fixed angular diameter, such as 20 arcsecond. The problem with such an approach is obvious and is illustrated in Figure 2-15. Two galaxies, with the same *linear* diameter but at different distances from Earth, are seen through the same aperture; the more distant galaxy (left) fits well within the aperture whereas parts of the nearer galaxy (right) fall outside it and do not, therefore, contribute to the measured magnitude.

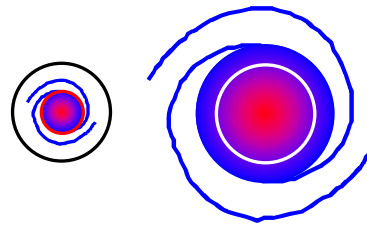


Figure 2-15. Metric magnitude.

The second method which is to measure the magnitude within a *standard isophote*, typically $\mu_B=25$ (de Vaucouleurs) or $\mu_B=26.5$ (Holmberg), where μ_B is the surface brightness in the *B* band. As the brightness of the night sky in the *B* band is typically 22 magnitudes per square arcsecond, you will realise that measuring out to these standard isophotes is no mean achievement.

Corresponding to these isophotes are the *de Vaucouleurs diameter* D_o – the diameter of the semi-major axis out to $\mu_B=25$ – and the *Holmberg radius* R_H – the radius of the semi-major axis out to $\mu_B=26.5$. Because $\mu(\theta, \phi)$ is independent of distance, absolute magnitudes and *angular* diameters deduced using this method are independent of the distance of the galaxy.

Measured total blue magnitudes range from ~ 10 (corresponding to $\sim 10^6 L_{\text{sun}}$) for dwarfs up to ~ -20 (corresponding to $\sim 10^{10} L_{\text{sun}}$) for large galaxies. The corresponding values of D_o range from ~ 1 kpc up to ~ 100 kpc.

3.3 Photometry of Elliptical Galaxies

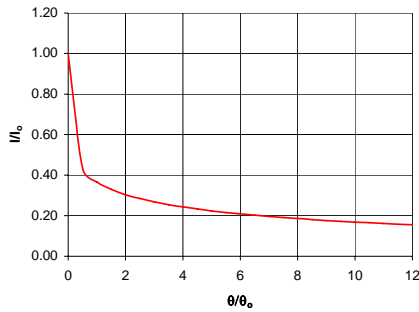


Figure 2-16. The de Vaucouleurs profile.

Let $I_E(\theta)$ be the surface brightness of an elliptical galaxy at a projected angular distance θ from its centre *along its major axis*. It is found that, for a large number of elliptical galaxies, $I_E(\theta)$ follows the *de Vaucouleurs* $\theta^{1/4}$ law:

$$I_E(\theta) = I_E(0) \exp \left[- \left(\frac{\theta}{\theta_{0E}} \right)^{1/4} \right], \quad (2.29)$$

where θ_{0E} is the angular distance at which the brightness has fallen to 1/e of its central value. This form of $I_E(\theta)$ is shown in Figure 2-16. To the extent that this law holds, it means that the light distribution in ellipticals can be described by two parameters, the central brightness $I_E(0)$ the scale-angle θ_{0E} . Note how, after an initial rapid drop, $I_E(\theta)$ falls off very slowly with angular distance from the centre; this is because the exponent depends only on the fourth root of θ .

Equation 2.25 is more usually written in the form:

$$I_E(\theta) = I_E(\theta_c) \exp \left\{ - 7.67 \left[\left(\frac{\theta}{\theta_c} \right)^{1/4} - 1 \right] \right\}. \quad (2.30)$$

The advantage of this form is that half the luminosity of the galaxy is emitted from within the “effective radius” θ_c . I shall continue to use the simpler form of 2.25 (2.29). Note that other laws can be found which fit the observed distribution just as well within the accuracy of observation; see [2], for example.

In terms of magnitudes, the de Vaucouleurs law 2.25 becomes a linear relationship in $\theta^{1/4}$:

$$\mu_E(\theta) = 1.086 \left(\frac{\theta}{\theta_{0E}} \right)^{1/4} + \mu_E(0). \quad (2.31)$$

Another successful fit for some ellipticals is the *Hubble-Reynolds law*, given by

$$I_H(\theta) = \frac{I_H(0)}{(1 + \theta/\theta_{0H})^2}. \quad (2.32)$$

We shall see later a natural explanation of this law.

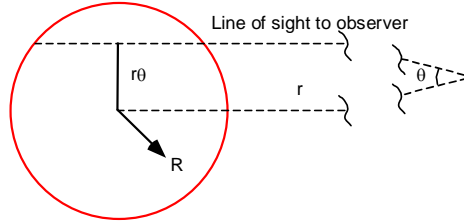


Figure 2-17. Projection on the sky.

You should realise that θ is a measure of the *projected* distance from the centre of the galaxy: at any given θ , we are seeing the radiation emitted from all points within the galaxy along the line of sight FN shown in Figure 2-17. What we really want to know is the luminosity $J(R)$ emitted *per unit volume* of the galaxy, as a function of the linear distance R from its centre. In general, the relationship between $J(R)$ and $I(\theta)$ is complicated but I shall illustrate a point by using a very simple case. Consider the so-called *modified Hubble profile* $I_h(\theta)$ for a spherically symmetric elliptical galaxy:

$$I_h(\theta) = \frac{I_h(0)}{1 + (\theta/\theta_{0h})^2}. \quad (2.33)$$

It can be shown – try it if you like! – that this corresponds to a *volume* intensity distribution $J_h(R)$ given by

$$J_h(R) = \frac{J_h(0)/R_{0h}}{[1 + (R/R_{0h})^2]^{3/2}}. \quad (2.34)$$

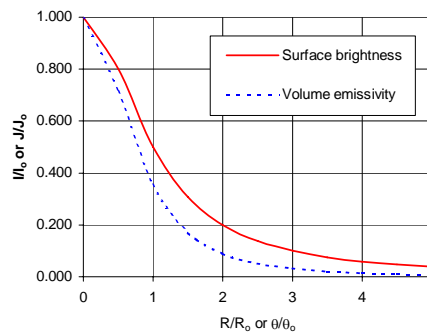


Figure 2-18. Surface and volume brightness.

Figure 2-18 shows $I_h(\theta)$ and $I_h(R)$ plotted on the same graph. You will see that $J_h(R)$ falls off *more rapidly* with θ than does $I_h(\theta)$. This is a *general* result: the

luminosity per unit volume of a galaxy is more concentrated towards the centre than the surface photometry (the *projected* luminosity). The generation of radiation is, therefore, more concentrated towards the centre of galaxies than is immediately apparent from the photometry. If we assume that the distribution of mass in stars follows the distribution of luminosity, we deduce that the mass of galaxies – in stars at least – is also more concentrated towards their central regions than appears from their surface brightness. We shall see later, though, that the distribution of *total* mass is not so concentrated.

It is easy to calculate the total flux-density F_E of an E0 galaxy from the de Vaucouleurs profile (2.29); the result is

$$F_E = 8! \pi \theta_{0E}^2 I_E(0). \quad (2.35)$$

More generally, for an EI galaxy, it is easy to show that

$$F_E = \left(1 - \frac{n}{10}\right) \times 8! \pi \theta_{0E}^2 I_E(0). \quad (2.36)$$

If, instead of obeying the de Vaucouleurs law, the brightness of an elliptical were uniform out to θ_{0E} and zero outside this angle, then the total flux would be given by

$$F_E = \pi \theta_{0E}^2 I_E(0). \quad (2.37)$$

A real elliptical therefore radiates $8!$, or approximately 40,000, times as much as a uniform disc of radius θ_{0E} ! This is because the intensity falls off rather slowly with distance from the centre of the galaxy, and the outer regions of the galaxy, - whose areas are bigger - contribute a lot of flux.

3.4 Photometry of Spiral Galaxies

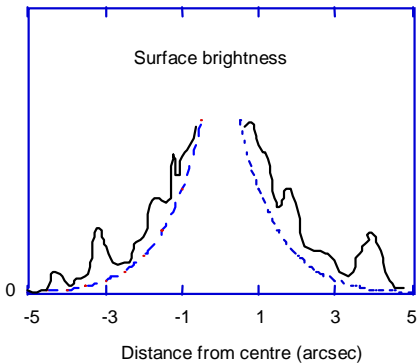


Figure 2-19. Surface brightness of disc galaxy.

I shall first consider spiral galaxies with no distinctive nuclear spheroidal component, that is late Sc or Scd galaxies. Of course we tend to think that most of the brightness of the discs of spirals comes from the spiral arms. To some extent this is a trick of the brain; in fact, there is a substantial brightness *underlying* the arms as

is shown schematically by the dotted curve in figure Figure 2-19, which is a schematic photometric scan across an Sc galaxy.. The difference between the full and dotted curves in this figure represents the contribution of the arms. The average underlying distribution $I_D(\theta)$ disc of a spiral galaxy is well described by the equation⁶

$$I_D(\theta) = I_D(0) \exp\left(-\frac{\theta}{\theta_{0D}}\right), \quad (2.38)$$

that is, an exponential expression in the *first* power of the radius θ . Again it is a remarkable result and means that the light distribution of the underlying spiral disc can be described by two parameters, the central brightness $I_D(\theta)$ and the scale-factor θ_{0D} . Because we are dealing with a flat disc, there is no essential difference between $I_D(\theta)$ and the luminosity emitted per unit volume of the disc. Equation (2.50) may also be taken, therefore, as representing the luminosity per unit volume as well as that per unit surface area. In terms of magnitudes, we have from equations (2.24) and (2.57),

$$\mu_D(\theta) = -2.5 \log \left[\frac{I_D(\theta)}{I_0} \right] = 1.086 \left(\frac{\theta}{\theta_{0D}} \right) + \mu_D(0), \quad (2.39)$$

where

$$\mu_D(0) = -2.5 \log \left[\frac{I_D(0)}{I_0} \right]. \quad (2.40)$$

It is easy to show that the total flux density F_D of a spiral's disc is given by

$$F_D = 2\pi \theta_{0D}^2 I_D(0). \quad (2.41)$$

Unlike an elliptical galaxy (cf. equation (2.35)), the disc of a spiral radiates only twice the flux of a uniform disc of radius θ_{0D} . This is because of the much faster fall-off of the disc's brightness with radius. The effect is even noticeable to the eye in photographs: spiral discs seem to come to an end much more abruptly than do elliptical galaxies. It is therefore somewhat less risky to use the brightness profiles to estimate the total luminosity of spirals than it is for ellipticals.

What happens if we add a nuclear spheroidal component to the disc? Perhaps not too surprisingly, we find that the total brightness distribution $I_S(\theta)$ is the sum of a term like (2.29) for the nucleus and one like (2.29) for the disc:

$$\mu_S(\theta) = \mu_N(\theta) + \mu_D(\theta) \quad (2.42)$$

where the intensity $I_N(\theta)$ the nuclear bulge is given by

⁶ For simplicity, I consider only face-on discs. The results can easily be generalised.

$$I_N(\theta) = I_N(\theta) \exp \left[- \left(\frac{\theta}{\theta_{0N}} \right)^{1/4} \right]. \quad (2.43)$$

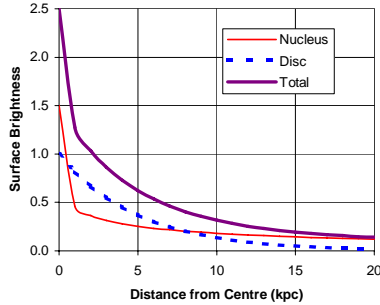


Figure 2-20. Brightness of nucleus and disc of spiral.

These two contributions in an imaginary Sc galaxy are shown schematically in Figure 2-1, which also shows the total surface brightness of the galaxy (excluding the arms). The scale-factor for the disc of this galaxy is 5 kpc and that for the nucleus is 0.5 kpc.

The relative contributions of the nuclear bulge and the disc components of spirals vary enormously along the Hubble sequence, from Sa to Scd. The scale-length R_{0D} for the discs of spirals is in the range of about 1 to 5 kpc; the corresponding length R_{0N} for the bulge can be very much less. As the figure shows, though, this does not mean that the brightness of the nucleus falls off rapidly compared with the disc; the one-fourth power dependence in the nuclear exponent gives it a much lower rate of fall-off.

It appears from the above discussion that, as far as the light distribution goes, we may regard a spiral as a disc surrounding a nuclear component that is rather like an elliptical galaxy. I shall show that there are other similarities between elliptical galaxies and the nuclear bulges of spirals, although there are differences too. You will not be surprised that lenticular galaxies have a similar behaviour to that of spirals.

3.5 Colours of Galaxies

Figure 2-21 is a schematic colour-colour plot of various types of galaxy. Also plotted is the locus of the colours of stars of different spectral types and the locus of the colours of blackbodies of various temperatures. The plot shows that elliptical galaxies are redder than spirals and that spirals get bluer as we move along the Hubble sequence from Sa through Sd to Magellanic irregulars. Note that, unlike stars of a particular spectral type, galaxies of a particular Hubble type occupy a broad region of the diagram. This reflects the fact that each galaxy is made up of a range of stars of different spectral types; the trend amongst the Hubble types is the result of different proportions of these stars.

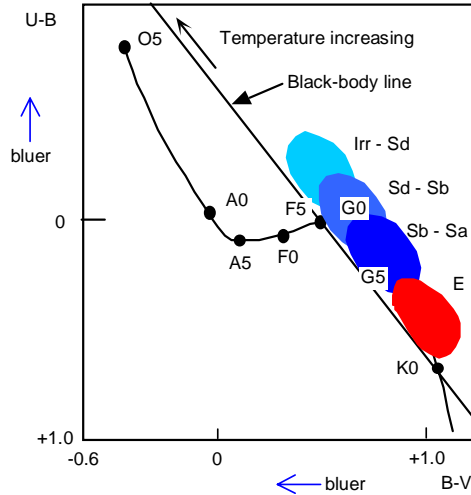


Figure 2-21. Colour-colour plot for galaxies.

On the whole, redder colours mean older stars so that *on the whole* the stars in E and S0 galaxies are older than those in spirals. Baade divided stars into Population I (Pop I), which are young, and Population II (Pop II) which are old⁷. We may conclude that ellipticals, lenticulars and the bulges of spirals consist predominantly of Pop II. The discs of spirals, on the other hand, contain many Pop I stars. Remember, however, that we are taking averages; we shall see later that there are stars in spirals that are just as old as those in ellipticals. More detailed study of the stars in galaxies confirms the above evidence of the colour photometry.

4. Masses of Galaxies

4.1 Introduction

Knowing the masses of galaxies is important both for the study of galaxies themselves and for cosmology, where we want to be able to estimate the mean density of the universe. There are two basic methods of estimating galaxian masses – by photometry and by spectroscopy. The photometric method assumes that we know the *mass-to-light ratio*, or *mass-luminosity ratio* of luminous material: given the photometry (or surface photometry) of a galaxy, we can estimate its mass (or distribution of mass) using the mass-to-light ratio. The spectroscopic methods use the Doppler effect to study the dynamics of a galaxy. We then deduce the distribution of mass within the galaxy needed to produce these dynamics.

Unfortunately, the two methods do not give consistent results, an example of the so-called *dark-matter problem*. Part of the reason for this is obvious: any method which depends on using mass-luminosity ratios to estimate mass will inevitably miss any *non-luminous* matter which may be present. Even within a given method, however, there are also discrepancies.

⁷This is an oversimplification but serves our purpose here.

4.2 Photometric Methods

4.2.1 MASS-LUMINOSITY RATIOS FOR STARS

As I said above, this method depends on knowing the mass-luminosity (M/L) ratio of galaxies. There is a danger of going round in a circle here: to know M/L for a particular galaxy, we need to know its luminosity *and* its mass! We can, however, use observations within our own galaxy to get Galactic values of M/L and assume that we can extrapolate these values to other galaxies.

One value of M/L we know very well is that of the sun^{8, 9}:

$$\frac{M_{\text{sun}}}{L_{\text{sun}}} = \frac{1.989 \times 10^{30} \text{ kg}}{3.826 \times 10^{26} \text{ W}} = 5.119 \times 10^3 \text{ kg W}^{-1}. \quad (2.44)$$

It is very convenient in astronomy to use solar values as the standard units. Let us define the dimensionless quantity M as the ratio of the mass M of an object to that of the sun:

$$M := M/M_{\text{sun}}. \quad (2.45)$$

Similarly, define the dimensionless luminosity L of an object of luminosity L as

$$L := L/L_{\text{sun}}. \quad (2.46)$$

Then the mass-luminosity ratio of the object can be expressed in the dimensionless form M/L :

$$\frac{M}{L} = \frac{(M/M_{\text{sun}})}{(L/L_{\text{sun}})} = \frac{[M(\text{kg})/L(\text{W})]}{5.119 \times 10^3 \text{ kg W}^{-1}}. \quad (2.47)$$

The value of M/L varies by many orders of magnitudes for main-sequence stars, as shown in **Table 2-1**.

Table 2-2. Mass-luminosity ratios of stars.

Spectral Type	M/L
O5	$\sim 10^{-5}$
A0	~ 0.04
K5	~ 4.4
M5	30

How, then, do we predict the mass-luminosity ratio of a collection of stars of various classes such as we have in galaxies?

⁸Note that I am using the *bolometric* luminosity of the sun. We more usually measure the luminosity of an object in some restricted wavelength range such as the B band. I shall not usually make this distinction.

⁹The usual symbol for the sun is \odot . Unfortunately, I do not seem able to force it into equations!

4.2.1 STELLAR MASS-FUNCTION

Let $N(M)$ be the number of stars per unit volume with mass greater than M . The number $\phi(M)dM$ with masses in the range M to $M + dM$ is then given by

$$\phi(M)dM = -\frac{dN(M)}{dM}dM. \quad (2.48)$$

In the solar neighbourhood, which is clearly not typical of all galaxian environments but which I shall use for illustration, we find that

$$\phi(M) = \phi_* \left(\frac{M}{M_*} \right)^{-\alpha}; \quad \alpha \sim 2.5, \quad (2.49)$$

where M_* is some characteristic mass and ϕ_* is the value of $\phi(M)$ at M_* . Because of the negative exponent in equation (2.49), the distribution is dominated by *low*-mass stars. Indeed, the total number N_{total} of stars of masses between the lower mass-limit M_{low} and the upper mass-limit M_{high} for stars is given by

$$\begin{aligned} N_{\text{total}} &= \int_{M_{\text{low}}}^{M_{\text{high}}} \phi(M) dM = \phi_* \int_{M_{\text{low}}}^{M_{\text{high}}} \left(\frac{M}{M_*} \right)^{-\alpha} dM \\ &= \frac{\phi_* M_*}{(1-\alpha)} \left[\left(\frac{M_{\text{high}}}{M_*} \right)^{1-\alpha} - \left(\frac{M_{\text{low}}}{M_*} \right)^{1-\alpha} \right] \\ &= \frac{\phi_* M_*}{(\alpha-1)} \left(\frac{M_{\text{low}}}{M_*} \right)^{1-\alpha} \left[1 - \left(\frac{M_{\text{low}}}{M_{\text{high}}} \right)^{\alpha-1} \right] \\ &\approx \frac{\phi_* M_*}{(\alpha-1)} \left(\frac{M_{\text{low}}}{M_*} \right)^{1-\alpha}, \end{aligned} \quad (2.50)$$

where the last line follows because $\alpha > 1$ and $M_{\text{high}} \gg M_{\text{low}}$. Equation (2.50) shows that the total number of stars is very sensitive to the uncertain lower-mass limit M_{low} , diverging as M_{low} tends to zero.

The total mass M_{total} all the stars is also dominated by the low-mass stars because

$$\begin{aligned} M_{\text{total}} &= \int_{M_{\text{low}}}^{M_{\text{high}}} \phi(M) M dM = \phi_* M_* \int_{M_{\text{low}}}^{M_{\text{high}}} \left(\frac{M}{M_*} \right)^{1-\alpha} dM \\ &\approx \frac{\phi_* M_*^2}{(\alpha-2)} \left(\frac{M_{\text{low}}}{M_*} \right)^{2-\alpha}, \end{aligned} \quad (2.51)$$

since $\alpha > 2$. This again diverges as M_{low} tends to zero.

What about the total luminosity L_{total} ? On average, the luminosity of a main sequence star is proportional to its mass to the power 3.3:

$$L(M) = L_* \left(\frac{M}{M_*} \right)^{3.3}, \quad (2.52)$$

where L_* is the luminosity of a star of mass M_* . Using the same approach as above, we get

$$\begin{aligned} L_{\text{total}} &= \int_{M_{\text{low}}}^{M_{\text{high}}} \phi(M) L(M) dM \\ &= \phi_* L_* \int_{M_{\text{low}}}^{M_{\text{high}}} \left(\frac{M}{M_*} \right)^{3.3-\alpha} dM \\ &\approx \frac{\phi_* M_* L_*}{(4.3-\alpha)} \left(\frac{M_{\text{high}}}{M_*} \right)^{4.3-\alpha}, \end{aligned} \quad (2.53)$$

since $\alpha < 4.3$. It is clear that, in contrast to the total mass, the total luminosity is controlled by the (equally uncertain) *upper* mass-limit. Combining the results of equations (2.51) and (2.53), we see that the mass-luminosity ratio in the solar neighbourhood depends on *both* the uncertain mass limits:

$$\begin{aligned} \frac{M_{\text{total}}}{L_{\text{total}}} &\approx \left(\frac{4.3-\alpha}{\alpha-2} \right) \times \left(\frac{M_*}{L_*} \right) \times \left(\frac{M_*^{2.3}}{M_{\text{high}}^{4.3-\alpha} M_{\text{low}}^{\alpha-2}} \right) \\ &\propto \frac{1}{M_{\text{high}}^{4.3-\alpha} M_{\text{low}}^{\alpha-2}} \approx \frac{1}{M_{\text{high}}^{1.8} M_{\text{low}}^{0.5}} \end{aligned} \quad (2.54)$$

Best estimates give

$$\left(\frac{M}{L} \right)_{\text{total}} \sim 2. \quad (2.55)$$

As we shall see, this is much lower than the values given by dynamical methods.

4.3 Spectroscopic Methods

4.2.1 PHYSICAL BASIS

All spectroscopic methods depend ultimately on measuring some characteristic velocity associated with some component of the galaxy and assuming that this velocity is determined by the galaxy's gravitational field. Even without going into more detail than this, it is simple to deduce from dimensional arguments that the mass M of a galaxy in which the characteristic velocity v is observed must be given by

$$M = \beta \frac{Rv^2}{G}, \quad (2.56)$$

where R is the characteristic size of the galaxy (or component), G the gravitational constant and β is a numerical constant. Of course, relation (2.56) will not give the value of β and it begs the question of what is meant by the characteristic size and velocity. Nonetheless, we shall see the general form of the

relationship appearing in all estimates of mass, as indeed it must because it involves all the relevant quantities and is dimensionally correct.

There are basically three methods: use of the virial theorem for elliptical galaxies and galaxies in clusters; (statistical) use of Kepler's equations for binary galaxies; and use of orbital dynamics for spiral galaxies.

4.3.1 THE VIRIAL THEOREM

For a *bound* self-gravitating system – that is one in which has negative total energy – the virial theorem states that the average, over an infinite time, of the sum of twice the kinetic energy T and the potential energy Ω is zero:

$$\lim_{\tau \rightarrow \infty} \left\{ \frac{1}{\tau} \int_0^{\tau} [2T(t) + \Omega(t)] dt \right\} = 0 \quad (2.57)$$

Unfortunately, we cannot wait an infinite time, or even for a time which is large compared to the time-scales on which things move around galaxies (typically 10^8 y). I shall show later, however, that the individual stars in galaxies (and to some extent galaxies in clusters) move more or less independently of other *individual* stars and only respond to the *overall* – essentially constant – gravitational field produced by the others. The total energy of an isolated system must remain constant and therefore, if the potential energy is effectively constant, the total kinetic energy must also be more or less independent of time. We can therefore approximate the ensemble averages of the kinetic and potential energies in equation (2.57) their *actual* values at the time of observation, giving

$$2T + \Omega \approx 0. \quad (2.58)$$

Let us use this to determine the masses of elliptical galaxies.

4.3.2 MASSES OF ELLIPTICAL GALAXIES

The first problem is to determine Ω . Using dimensional arguments, we can deduce that

$$\Omega = -\alpha \frac{GM^2}{R}, \quad (2.59)$$

where M is the mass of the galaxy contained within some characteristic distance R and α is a dimensionless numerical constant which depends upon the distribution of mass within the galaxy. It can be shown that, for a uniform, spherically symmetric distribution, $\alpha = 3/5$. The calculation of α is more difficult for non-spherical distributions and requires assumptions about the variation of the density, which has to be derived from the light distribution (see above). Moreover, as I have already pointed out, we do not know the true shape of elliptical galaxies. Fortunately a few trial cases of reasonable density distributions is enough to convince us that the value of α is always close to unity.

The next step is to estimate $2T$, twice the kinetic energy of the stars. Obviously the kinetic energy of a star is a function of its velocity and this in turn can be measured using the Doppler shift of its spectral lines. If star i has mass m_i and velocity v_i , its kinetic energy T_i is given by

$$T_i = \frac{1}{2} m_i v_i^2 \quad (2.60)$$

so that T , the total energy of the N stars in the galaxy, is given by

$$T = \sum_{i=1}^N \frac{1}{2} m_i v_i^2. \quad (2.61)$$

We can get an *approximate* expression for T by writing

$$\sum_{i=0}^N m_i v_i^2 \approx N \langle m \rangle \langle v^2 \rangle \quad (2.62)$$

where $\langle \rangle$ denotes an average over all the stars in the galaxy. Hence

$$2T \approx M \langle v^2 \rangle, \quad (2.63)$$

where M is the total mass of stars of the galaxy, because the average mass $\langle m \rangle$ of the stars is defined by

$$\langle m \rangle = \frac{M}{N}. \quad (2.64)$$

Combining equations (2.57), (2.59) and (2.63), I get

$$M \approx \frac{R \langle v^2 \rangle}{\alpha G}. \quad (2.65)$$

Equation (2.65) has the same form as (2.56) which, of course, it must.

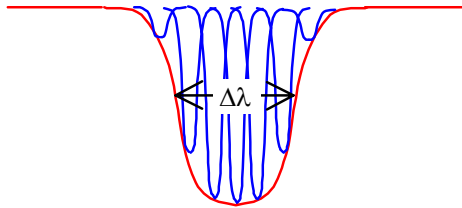


Figure 2-22. Schematic view of galaxian absorption line built up of the lines of individual stars.

How can we estimate $\langle v^2 \rangle$? The spectrum of each star in the galaxy will show the absorption lines of the star's atmosphere. Because the stars are moving with respect to each other, these absorption lines will be Doppler-shifted one with another. Relative to the rest-frame of the galaxy, the shift $\delta\lambda_i$ of a line in star i 's spectrum is given by

$$\frac{\delta\lambda_i}{\lambda_i} = \frac{v_{r,i}}{c}, \quad (2.66)$$

where $v_{r,i}$ is the line-of-sight velocity of the star and c is the velocity of light. As there are some 10^{11} stars in a large elliptical galaxy, it is not possible to measure the line-of-sight velocity of each star individually! Because there is a range of stellar velocities, however, there is a spread in the Doppler shifts of their individual lines. Most of the stars will be moving relatively slowly and therefore contribute a lot of absorption with nearly zero Doppler shift. Fewer stars will be moving fast and so there will be less absorption at higher shifts. The overall effect, shown schematically in Figure 2-22, is to broaden the absorption line from the galaxy as a whole.

The overall width $\Delta\lambda$ of the line is given by

$$\Delta\lambda \equiv \langle \delta\lambda_i^2 \rangle^{1/2} = \lambda \frac{\langle v_{r,i}^2 \rangle^{1/2}}{c} \quad (2.67)$$

where, as before, $\langle \rangle$ denotes an average over all the stars in the galaxy.

Because the Doppler effect only gives us the line-of-sight velocity of the star, we need to make some assumption about the two components of velocity perpendicular to that line of sight¹⁰. I shall make the simplest assumption that the mean-squares of the components of the velocities in every direction are approximately the same¹¹ so that

$$\langle v_{r,i}^2 \rangle \approx \langle v_{p1,i}^2 \rangle \approx \langle v_{p2,i}^2 \rangle, \quad (2.68)$$

where $v_{p1,i}$ and $v_{p2,i}$ are two orthogonal components of the star's velocity perpendicular to the line of sight. Then

$$\langle v_i^2 \rangle \equiv \langle v_{r,i}^2 + v_{p1,i}^2 + v_{p2,i}^2 \rangle \approx 3 \langle v_{r,i}^2 \rangle \quad (2.69)$$

From equations (2.65), (2.67) and (2.69), we get

$$M \approx \frac{3}{\alpha} \frac{R \langle v_{r,i}^2 \rangle}{G} = \frac{3}{\alpha} \frac{R c^2}{G} \left(\frac{\langle \delta\lambda_i^2 \rangle^{1/2}}{\lambda} \right)^2. \quad (2.70)$$

I have gone through this rather lengthy argument in some detail for two reasons. First, it is fundamental to determining the masses, both of individual (elliptical) galaxies and of galaxies in clusters. Secondly, you should understand the assumptions and approximations involved and realise the uncertainty of all our estimates

¹⁰Proper motions could, in principle, give us this information but the proper motion of stars in other galaxies is far too small to be detected.

¹¹This is obviously unlikely to be true in galaxies with marked ellipticity; for a sample of galaxies, this can be corrected for statistically.

of mass. A last point is worth making. Like all methods of estimating mass, it delivers only the mass within some radius R , out to which the measurements have been made. There is no guarantee that there is not more mass outside this distance.

The estimated masses of elliptical galaxies range from $10^6 M_{\text{sun}}$ for dwarfs to over $10^{12} M_{\text{sun}}$ for giants. The lower end of the range overlaps with that of globular clusters of stars in our own galaxies.

4.3.3 MASSES OF SPIRAL GALAXIES

In assuming that the three components of velocity in elliptical galaxies were the equal, I rejected any possibility of large-scale systematic motion. For spiral galaxies, on the other hand, it is clear that material is in large-scale rotation about the centre of the galaxy. This was deduced long ago for our own Galaxy from observations of the motion of nearby stars relative to the sun; it has been confirmed by radio observations of material, such as neutral hydrogen (HI) atoms and molecules like CO, distributed throughout the Galaxy. In other galaxies the same techniques can be used: the line-of-sight velocity of stars or gas in the disc of the galaxy can be deduced from the Doppler shift of lines and this line-of-sight velocity converted into a velocity of motion about the centre of the galaxy. In doing this, we assume that the disc material is essentially in circular orbit about the centre of the galaxy, an assumption I shall justify later.

There are conflicting requirements on the orientation of galaxies suitable for measuring rotational velocities. In order to see clearly from what part of a galaxy a particular line originates, we should prefer the galaxy to be as face-on to us as possible. Unfortunately, the material in a face-on galaxy has essentially no line-of-sight component of velocity and so there is no Doppler shift! The *maximum* shift is obtained principle from an edge-on galaxy but there are two problems with such an orientation. First, we have to look *through* the material of an edge-on disc. Many disc galaxies have dust lanes that will obscure starlight so that only radio lines from interstellar gas can be used. In any case, the line-of-sight passes through material that is at a range of distances from the centre of the galaxy and is hence moving at a range of velocities, making interpretation difficult. We need to compromise, choosing galaxies which are sufficiently inclined to allow us to resolve where in the disc the lines are coming from whilst still giving appreciable components of velocity in the line of sight.

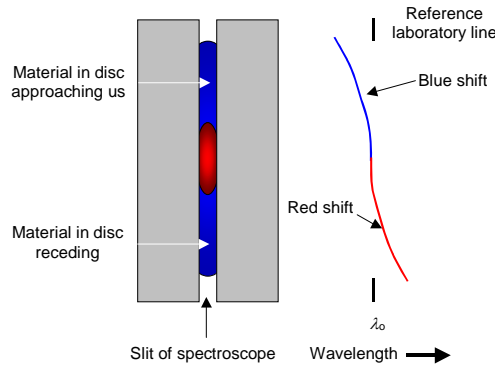


Figure 2-23. Long-slit spectroscopy.

Figure 2-23 shows schematically how long-slit spectra are used to measure a galaxy's rotation curve in the optical. The slit of the spectrograph is placed along the major axis of the galaxy as shown. The resultant spectrum of a single line of rest-wavelength λ_0 is shown on the right, relative to the same line produced by a laboratory source. The parts of the galaxy which are approaching the observer give rise to blue shifted lines whilst those which are receding give rise to red-shifted lines. The overall effect is to produce the curved spectral line shown in (exaggeratedly) the figure¹².

Let $\Theta(r)$ (called the *circular velocity*) be the velocity of rotation – in circular orbit about the centre of a galaxy – of the material at distance r from the centre of the galaxy. Then, neglecting the inclination of the galaxy to the line of sight, for simplicity, we get for the wavelength shift $\Delta\lambda$ as a function of r ,

$$\frac{\Delta\lambda}{\lambda_0} = \frac{\Theta(r)}{c} \tag{2.71}$$

A plot of the circular velocity against the distance from the centre of the galaxy is called a *rotation curve*. A schematic example is shown as the solid curve in Figure 2-24. Note that, after an initial rise from the centre of the galaxy, the rotation curve is rather flat; this is typical of the majority of spirals. Indeed, the curves usually remain flat as far out as matter can be traced, using radio and millimetre techniques.

¹²For simplicity, I have assumed that the galaxy as a whole is at rest with respect to the Earth. In practice, the centre of the line would also be red-shifted with respect to the laboratory line because of the galaxy's recession.

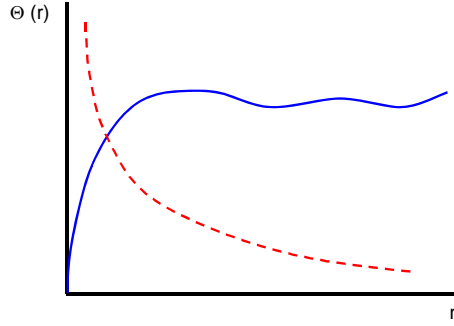


Figure 2-24. Rotation curve of spiral galaxy.

Given the rotation curve, we can attempt to construct a model of the distribution of mass that would give rise to that curve. The simplest assumption, which turns out to be rather good for the outer regions of galaxies, is that the material is distributed in a *dark halo* with spherical symmetry about the centre of the galaxy. This is surprising in view of the very obvious concentration of *visible* matter in the plane of the galaxy; I shall return to this point shortly. It is fortunate for us, though, because the gravitational field of a spherically symmetric distribution of matter is easy to calculate whereas that of a disc is much more difficult.

We shall deal with circular motion in disc galaxies in more detail in Chapter III. I want only to consider some elementary results here. For a *spherically symmetric* distribution of matter, the motion at distance r from the centre depends only upon the mass $M(r)$ contained within r . For the circular velocity $\Theta(r)$ of a star of mass m I can, therefore, write

$$\frac{m\Theta^2(r)}{r} = \frac{GM(r)m}{r^2}, \tag{2.72}$$

which just says that the centripetal acceleration is provided by the gravitational force. If essentially all the mass of the galaxy were concentrated at its centre, then we should have

$$M(r) = M(0) = \text{constant}, \tag{2.73}$$

in which case we should have from equation (2.72) that the rotation curve would be given by

$$\Theta(r) = \left[\frac{GM(0)}{r} \right]^{1/2} \propto r^{-1/2}. \tag{2.74}$$

This is Keplerian rotation shown as the dashed curve in Figure 2-24. Obviously a model in which all the mass is concentrated at the centre does not adequately represent a real spiral galaxy.

From equation (2.72), we can immediately obtain an expression for the mass $M(r)$ contained within r :

$$M(r) = \frac{r\Theta^2(r)}{G}, \tag{2.75}$$

Let us first look at the flat outer part of the rotation curve. If we put, as a first approximation to the rotation curve,

$$\Theta(r) \approx \Theta_0 = \text{constant}, \tag{2.76}$$

we see immediately from equation (2.75) that

$$M(r) = \frac{r\Theta_0^2}{G} \propto r. \tag{2.77}$$

Observation of molecular gas has enabled the rotation curves of many galaxies to be measured out to several times the radius of the optically visible disc. Remarkably, only in a few cases do these curves *show any sign of falling off* from a constant Θ_0 , as indicated in Figure 2-24. Thus, according to relation (2.77), the mass of the galaxy continues to grow as far as out we can trace it! Any estimate we make of the total mass of the galaxy can therefore only be a lower limit. A second problem is that the masses involved are much as an order of magnitude or more greater than that estimated by adding up the masses of the material which we can observe in stars and gas. This must be true, of course, if the mass is distributed with spherical symmetry because most of the observed material is in the disc. We have here another example of the “dark matter” problem.

Given the way that $M(r)$ depends upon r , we can work out what the density profile $\rho(r)$ must be. For the mass $dM(r)$ contained between r and $r + dr$ we have

$$dM(r) = 4\pi r^2 dr \times \rho(r) \tag{2.78}$$

so that

$$M(r) \equiv \int_0^r dM(r') = 4\pi \int_0^r \rho(r') r'^2 dr'. \tag{2.79}$$

Let us assume that $\rho(r)$ takes the power-law form

$$\rho(r) = \rho_0 \left(\frac{r}{r_0} \right)^\alpha. \tag{2.80}$$

Then it is easy to show that $M(r)$ is given by

$$M(r) = \frac{4\pi}{(3+\alpha)} r_0^3 \rho_0 \times \left(\frac{r}{r_0} \right)^{3+\alpha}. \tag{2.81}$$

Comparing equations (2.77) and (2.81), we see that, to agree with observation of the outer parts of the galaxy, we must have

$$3 + \alpha = 1 \quad \text{or} \quad \alpha = -2, \tag{2.82}$$

so that the density falls off as the inverse square of the distance r from the centre of the galaxy.

Estimates of the masses of spiral galaxies, within a hundred parsecs or so of their centres, range from about $10^{10} M_{\text{sun}}$ to about $10^{12} M_{\text{sun}}$.

4.4 Mass-Luminosity Ratios for Galaxies

Putting together the results of photometry and the estimates of galaxian masses, we estimate the mass-luminosity ratio M/L for galaxies. We find:

$$\frac{M}{L} \sim \begin{cases} 20 - 40 h & \text{ellipticals} \\ 10 h & \text{spirals} \end{cases} \quad (2.83)$$

You should compare these values of M/L with the value of about 2 given above for stars. Once again, we see the need for *dark matter*. One possibility is that the halo consists largely of *brown dwarfs*, “stars” with masses less than about $0.05 M_{\text{sun}}$. These objects are not massive enough for nuclear reactions to start up in their centres and they derive their faint luminosity from slow gravitational contraction. They are expected to be cool objects, radiating most of their power in the infrared, and have been discovered recently *inter alia* by ESA’s *Infrared Space Observatory* (ISO) [e.g. 3]. Another possibility is that the matter is made up of white dwarf stars [4]. We shall see later, however, that not all dark matter in the universe can be in the form of normal baryonic material so the dark halos of galaxies may be dominated by exotic matter.

Bibliography for Note 2

- [1] Press Release number STScI-PR97-34
- [2] Binney, J and Merrifield, M. *Galactic Astronomy*, Princeton University Press, 1998. ISBN0-691-02565-7
- [3] *ISO observations of candidate young brown dwarfs*
Comerón, F., Rieke, G.H., Claes, P., Torra, J. & Laureijs, R.J.,
A&A **335**, 522-532 (1998)
- [4] *Faint, Moving Objects in the Hubble Deep Field: Components of the Dark Halo.*
Ibata, R A, Richer, H B, Gilliland, R L and Scott, D.
ApJ **524** L95-L97 (1999)